Raman spectroscopic analysis of the effect of annealing on hydrogen concentration and microstructure of thick hot wire grown a-Si:H films aimed as precursor layers for crystallized thin film silicon

S. Kurth[1*], W. Wang[1], V. Nickich[2], F. Pennartz[1], S. Haas[1], M. Nuys[1], W. Beyer[1]**

[1] IEK-5 Photovoltaik, Forschungszentrum Jülich GmbH, Wilhelm-Johnen-Str., 52428 Jülich, Germany

[2] CIRE, Technische Hochschule Köln, Claudiusstr. 1, Köln, Germany

[*] Corresponding author, contact: si.kurth@fz-juelich.de, telephone +49 2461 61 9733, fax +49 2461 61 3773

** current address: CNITECH, Ningbo Institute of Industrial Technology, No. 1219 Zhongguan West Road, Ningbo, China

Abstract For application as precursor layers for silicon solar cells fabricated by laser liquid phase crystallization, thick amorphous silicon films on glass are of interest. However, for hydrogenated amorphous silicon (a-Si:H) precursor layers containing about 10 at.% hydrogen, hydrogen needs to be removed prior to liquid phase crystallization to avoid bubble formation and peeling. For this purpose, an at least 12 hours annealing procedure up to 550°C is considered necessary thus involving long process time and high costs. In this article, we investigate the use of thick hot wire grown a-Si:H films which turn out to need considerably less time for dehydrogenation than dense plasma-grown a-Si:H. The dehydrogenation process is studied by depth profiles of hydrogen concentration and medium range order (MRO) using Raman spectroscopy analysis at etch pits. The results show already at an annealing temperature of 450°C the disappearance of all detectable H in the substrate-near part and the complete removal of H at 550°C after about 4 hours annealing. We attribute this rather fast hydrogen

removal to the formation of interconnected voids primarily in the substrate-near range. In the same range of the film, we find a correlation between hydrogen concentration and medium range order suggesting that a silicon network reconstruction due to hydrogen out-diffusion causes an observed decrease of reciprocal MRO. The results stress the importance of void-related microstructure in the a-Si:H for hydrogen removal at a rather low annealing temperature and short annealing time. Our results suggest that hot wire a-Si:H films which can be grown with a high deposition rate and a rather pronounced void-related microstructure may be well suited as economic precursor layers.

Keywords

Hydrogenated amorphous silicon, hydrogen concentration, medium range order, microstructure, Raman spectroscopy, liquid phase crystallization

1. Introduction

Crystallized silicon is of interest for the fabrication of thin film solar cells [1]. In particular the laser liquid phase crystallization (LLPC) of amorphous silicon is a promising as well as low-cost technology to prepare high quality crystalline silicon solar cells on inexpensive glass substrates [2]. Amorphous silicon precursor layers for LLPC which need to be rather thick in order to assure full absorption of sunlight by the crystallized silicon films can be fabricated by several methods, like from silane (SiH_4) based gas mixtures by plasma-enhanced chemical vapor deposition or by hot-wire chemical vapor deposition (HWCVD) as well as from solid silicon targets by electron beam physical vapor deposition. Due to its rather high potential deposition rate [3, 4] and compatibility with large area deposition techniques, HWCVD a-Si:H was chosen for our investigations. However, the incorporation of hydrogen of the order of 10 at.% into such hydrogenated amorphous silicon (a-Si:H) precursor layers can

lead to a decohesion/ peeling of the layer during the crystallization process [5]. Hence, the hydrogen needs to be removed from the precursor layers by annealing prior to the crystallization step [5, 6]. For thin a-Si:H films up to a thickness *d* of about 1 µm, the influence of annealing processes on the hydrogen concentration and its depth distribution has been rather intensively investigated [7-9]. Depending on deposition conditions it was found that a-Si:H grows as a quite dense or a more void-rich material. For films up to about 1 µm thickness, the void-related microstructure has also been investigated rather thoroughly using infrared absorption and Raman spectroscopy [8-10]. However, there is little information so far about the changes of H depth distributions upon annealing for thick films (d > 2 µm). In this work, depth-profiles of the hydrogen concentration, hydrogen related microstructure as well as medium-range order (MRO) are investigated by Raman spectroscopy. MRO is of interest as it describes the disorder in the amorphous silicon network caused by rotation of Si tetrahedra [11] and, therefore, can be expected to be sensitive to hydrogen removal by annealing. The results show that upon annealing up to 450°C, our thick (d ≈ 4.5 µm) a-Si:H film loses hydrogen in the substrate-near part of the film considerably more rapid than in the surface near range and expected for dense a-Si:H. The depth distributions of hydrogen concentration and medium range order are found to be correlated. From these experimental results we conclude that the 450°C annealing causes a structural change in the substrate near part of the film so that rather rapid motion of molecular hydrogen is involved in the H out-diffusion process. Due to the observed release of hydrogen at this quite low annealing temperature, we consider these HWCVD grown a-Si:H films of interest as precursor layers for liquid-phase crystallized thin film silicon solar cells.

2. Experimental Details

The a-Si:H precursor material was fabricated in a HWCVD deposition system equipped with tantalum filaments. The filament temperature during deposition was 1675 °C. The pressure of the SiH_4-H_2 gas mixture used was 5 Pa (0.05 mbar) with gas flows of 6 sccm SiH_4 and 6 sccm H_2. The typical film deposition rate was 0.5 nm/s. A substrate temperature of 200 °C was used. Under these deposition conditions, the hydrogen concentration as measured by infrared spectroscopy was approximately 10 at.%. As substrate, Corning glass (Corning Eagle XG, an alkaline earth boroaluminosilicate glass) was used, precoated with 220 nm SiOx, 70 nm SiNx and 10 nm SiOx ("ONO") by RF magnetron sputtering in this sequence. For the present work this ONO layer is of importance to enhance the sticking of the thick a-Si:H layers to the glass substrate [6]. For the final aim of thin film silicon solar cells on glass prepared by liquid phase crystallization, this ONO layer is of high importance as it fulfills a number of mechanical, optical and electronic functions. These involve, e.g., the function of wetting during liquid phase crystallization and acting as a diffusion barrier [6]. Much work has been devoted to ONO / intermediate layer development [12, 13].

In this work, we investigated three thick a-Si:H samples: one sample with a thickness of ~6000 nm stayed untreated (sample 1) while the other samples with a thickness of ~4500 nm were heated up to 450 °C (sample 2) and 550 °C (sample 3). We used three different samples instead of one (cut into pieces), since the cutting procedure often leads to a complete peeling of the film. Annealing was done in a vacuum oven with a base pressure of 2-4 x 10^{-4} Pa. Heating steps were applied as shown in Fig.1. The heating step at 350°C was applied as an intermediate heating step aimed to prevent peeling. We note that the peeling problems can likely be overcome by improved ONO /intermediate layers so that the heating procedure for a (solar cell) device can presumably be reduced to the highest temperature (4h) steps.

For depth-resolved investigation of the material properties by Raman spectroscopy [14], craters were etched into the a-Si:H layers reaching to the substrate. The etching was done using a 3 mol/l solution of potassium hydroxide in water. Raman-measurements were performed at the 250 – 350 µm wide sidewalls (wedges) of the 4.5 – 6 µm deep craters. A continuous-wave laser (Coherent Sapphire SF) with an emission wavelength of 488.05 nm was used for the excitation of the material. A laser power of 930 µW and a spot dimension of 50 µm x 2 µm was applied for the investigations. The longer side of the laser beam was oriented in parallel to the sidewall of the etching crater. The chosen laser wavelength leads to a Raman information depth of about 30 nm [10] for the as-deposited material. Using depth profiles of the craters measured with a Dektak instrument, the position of the laser spot was assigned to a depth d.

The Raman spectra show hydrogen-related structures in the range of 1900 – 2200 cm^{-1}. The structures are caused by stretching vibrations of Si-H bonds. As known from infrared absorption, the dispersion of the Raman spectra in this frequency range involves information on void-related microstructure [8, 10]. For evaluation of the hydrogen concentration from the Raman spectra we first subtracted the baseline which may originate from photoluminescence through oxidation of the surface [15]. Next, the spectra were normalized to the (Raman) peak intensity of the Si-Si TO vibrations of a-Si near 480 cm^{-1} [6]. Then the spectra were fitted by two Gaussians located near 2000 cm^{-1} (Si-H stretching mode in dense a-Si:H) and 2100 cm^{-1} (Si-H stretching mode of (void-) surface bound hydrogen) [16, 17], as demonstrated in Fig. 2. For both modes, the absorption was calculated by numerical integration of the respective fitted Gaussians. The sum of these integrals provides a measure of the ratio of hydrogen to silicon atoms, i.e. yielding a normalized Raman hydrogen intensity at a given depth. Since all spectra are normalized to the respective

Si-Si peak intensity near 480 cm^{-1}, the derived hydrogen intensity is independent of changes of the Raman laser intensity [6] and independent of annealing related changes of the a-Si:H optical bandgap which affects the Raman information depth. Thus, a comparison of Raman hydrogen intensity data for different samples and at different depths is possible and we refer to this Raman hydrogen intensity also as hydrogen concentration. Furthermore, the 2100 cm^{-1} and 2000 cm^{-1} Raman H intensities were used to define the hydrogen microstructure parameter R_H = I (2100 cm^{-1}) / ((I (2100 cm^{-1}) + I (2000 cm^{-1})) which is known to give information about void-related microstructure [10, 18].

The medium range order (MRO) microstructure describes the disorder/order in the amorphous silicon (Si-Si) network caused by rotation of Si tetrahedra inducing local network strain. Note that in the perfect crystalline silicon lattice, all Si tetrahedra are aligned with 0 ° rotational angle and there is, accordingly, no local lattice strain. For the characterization of the MRO microstructure, the intensity ratio of the area under the TA phonon near 150 cm^{-1} (I_{TA}) and the area under the TO phonon near 480 cm^{-1} (I_{TO}) was proposed, i.e. the MRO (microstructure) parameter is defined by MRO = I_{TA}/I_{TO} [19-22]. Thus, a high value of MRO is characteristic of a high disorder [19, 20] while MRO = 0 is valid for highly ordered crystalline silicon. Accordingly, MRO is valuable to describe the transition from amorphous to (micro-) crystalline silicon. For the characterization of microstructure of fully amorphous silicon, the parameter 1/MRO is more useful as it is proportional to the order in the material. Device grade a-Si:H shows high values of 1/MRO = 4-5 [22]. To our knowledge, the highest values reported for a-Si:H without microcrystalline inclusions were 1/MRO ≈ 5.2 [23, 24]. As shown in this article, driving out hydrogen by annealing often decreases 1/MRO and thus the order in the material. The reason is likely that the out-diffusion of

hydrogen which involves Si-Si bond reconstruction leads also to a rotation of the Si tetrahedra.

For evaluation of I_{TO}, the method described in [23] is used, as shown schematically in Fig. 3a. Here the peak assignment in terms of transversal acoustic (TA), longitudinal acoustic (LA), longitudinal optic (LO) and transversal optic (TO) modes of the amorphous Si-Si network is indicated [24]. The influence of the LO peak distorts the low frequency half of the TO peak. To account for this effect, we define medium range order (also termed the MRO microstructure parameter) in analogy to [23] by MRO = $I_{TA}/2(I_{TO}/2)$.

The effect of annealing on the a-Si Raman spectra in our a-Si:H material is illustrated in Fig. 3b for a depth of approximately 2650 nm from the surface. Annealing up to 550°C changes the position of the TO phonon peak only slightly, if at all, while the general features change considerably. Note that there is no indication for the formation of crystalline silicon which would show up as a Raman peak near 520 cm^{-1} [25]. What is also seen in Fig. 3b is the strong influence of the variation of the LO phonon near 400 cm^{-1} on the low energy (low wavenumber) side of the TO phonon near 480 cm^{-1}. This result supports the necessity for evaluation of the high energy side of this peak only. A related method for avoiding the contribution of the LO phonon has been proposed by Morell et al. [21]. They suggest to fit first the high frequency side of the TO phonon by a single Gaussian.

3. Results

The untreated sample (Fig. 4a) shows a relatively constant hydrogen concentration throughout the sample thickness. Also shown in Fig. 4a is the H microstructure parameter. The nearly constant value of $R_H \approx 0.2$ shows that the material contains some (void-) surface-bound hydrogen with its concentration nearly constant over the depth of the film. Annealing at 450 °C (Fig. 4b) changes the hydrogen depth profile significantly. Highly

surprising is the asymmetry of hydrogen concentration in the film. While the surface-near part of the film shows a maximum hydrogen concentration of about 25 % of the original value of the untreated sample, little to no silicon-bonded H could be detected in the range next to the substrate which is at the depth of about 4500 nm. For a-Si:H films of about 1 µm in thickness, both experimental [26, 27] and calculated [26-28] depth profiles of hydrogen show rather symmetric H out-diffusion towards film surface and film substrate interface. Highly surprising is, furthermore, the rather complete disappearance of hydrogen in the substrate-near range. For a dense a-Si:H material, the H diffusion coefficient has been measured and an Arrhenius dependence $D = D_0 \exp(-E_D/kT)$ was found with $E_D = 1.53$ eV and $D_0 = 1.17 \times 10^{-2}$ cm^2/s [29]. For the annealing temperature of 450°C a H diffusion coefficient of $D \approx 2.4 \times 10^{-13}$ cm^2 /s follows which results for an annealing time of 4h (ignoring the time-dependence of H diffusion [18, 30]) in a diffusion length ($L = 2(D\,t)^{½}$ of about 1.2 µm. For achieving the full depletion of H as found in the substrate-near part, a H diffusion length of at least the film thickness (≈ 4.5 µm) is needed which requires a H diffusion coefficient of about $D = 3.5 \times 10^{-12}$ cm^2/s, i.e. about a factor of 10 higher (or more) than in dense a-Si:H. To achieve a H diffusion length of 4.5 µm by annealing at 450°C for dense a-Si:H, an annealing time of almost 60h would be required. This result suggests that in the lower part of the film the motion of molecular H, which can be much faster than the diffusive motion of atomic H [18] plays a role. Both the asymmetry of the H concentration and the contribution of H_2 diffusion in the lower part suggest the formation of a void-related microstructure in the lower part of the film.

Fig. 4b also shows data of the H microstructure parameter. A value near $R_H \approx 0$ is found which can be explained (see Section 2) by the desorption of all surface bound hydrogen in the material for the annealing conditions applied. As $R_H \approx 0$ is observed throughout the annealed material, this desorption of H from void surfaces occurs not only in the substrate-near but also in the surface-near part of the film. We note that in literature for

a-Si:H with different microstructure after annealing both an increase of the 2000 cm^{-1} /2100 cm^{-1} absorption ratio (as found here) as well a decrease has been reported [30]. In hydrogen effusion measurements, desorption of surface bound hydrogen is known to show up as a peak near 400°C for a heating rate of 20°C/min [7]. Since any voids in the surface-near part of the films are unlikely interconnected, this hydrogen may be present within the material in the form of H_2.

The depth profile of the reciprocal microstructure parameter (1/MRO) of the as-deposited material is shown in Fig. 5a and of the material annealed at 450°C in Fig.5b. In the untreated sample (Fig. 5a), the 1/MRO is almost constant in depth, decreasing slightly from a value near 1/MRO ≈ 4 near the film surface towards a value of 1/MRO ≈ 3.7 at about 5000 nm depth. Close to the substrate (which is at a depth of 6000 nm), the low signal-to-noise ratio prohibits an evaluation of MRO. These values of 1/MRO ≈ 4 are close to the value of 1/MRO ≈ 4.2 reported for device-grade a-Si:H [22]. The reason for the slight depth dependence of 1/MRO is unknown so far. We note, however, that Morell et al. [21] and Danesh et al. [24] also observed higher 1/MRO values at the film surface compared to the bulk for plasma-deposited a-Si:H films when measured with strongly and weakly absorbed laser lines.

After annealing at 450 °C (Fig. 5b), the 1/MRO microstructure resembles strongly the dependence of H concentration on depth as shown in Fig 4b, i.e. exhibits a similar difference between the surface- and substrate-near parts of the film. In the upper (surface-near) part, a nearly constant 1/MRO with 1/MRO ≈ 3.9 is observed, dropping strongly at a depth exceeding about 2000 nm. A minimum of 1/MRO ≈ 2.8 is found at a depth near 3500 nm followed by some increase towards the film-substrate interface. The reduced values of 1/MRO in the lower (substrate-near) part of the film show a reduced order and appear consistent with the strongly reduced hydrogen content, as Si-Si bond

reconstruction due to hydrogen release is expected to cause a rotation of the silicon tetrahedra.

This similarity in the depth dependences of hydrogen concentration and 1/MRO parameter for the material annealed at 450°C suggests a correlation between 1/MRO and H concentration. Indeed, an almost linear dependence is found, as shown in Fig. 6. This result suggests that the more hydrogen is locally released, the more MRO disorder is generated. We explain this result by the reconstruction of Si-Si bonds throughout the amorphous material upon H release. In this process, the angle between the tetrahedra, i.e. MRO is expected to increase (network distortion) and the reciprocal MRO parameter to decrease. Qualitatively, our results agree with those by Pantchev et al. [30] who studied the effect of plasma post-hydrogenation on MRO of unhydrogenated sputtered a-Si films. An increase from 1/MRO = 2.08 to 2.94 was observed when a surface layer (about 10 nm) was post-hydrogenated to a hydrogen concentration of about 12 at.%. Both Pantchev´s and our results agree with the concept that incorporation of hydrogen (in dense a-Si:H) increases order while hydrogen removal causes the opposite.

Fig.7 shows the depth profile of 1/MRO for the sample annealed at 550 °C. Note that for this annealing state, no hydrogen could be detected in the material. 1/MRO decreases in Fig. 7 from a value 1/MRO ≈ 4 at the surface to about 3.3 at a depth exceeding 2 µm. One may explain the rather high value of 1/MRO near the film surface by a reduced Si network strain. Further within the film, the reduced values of 1/MRO are likely due to Si network reconstruction due to the release of hydrogen. For depths exceeding about 2 µm, the 1/MRO is found to be constant and up to 20 % higher than in the same depth range for the sample annealed at 450 °C. This may indicate some reordering of the silicon network at high annealing temperatures after hydrogen has completely diffused out. Annealing effects in the silicon network structure of unhydrogenated a-Si are known in this annealing temperature range exceeding 400°C

[32]. An increase of 1/MRO from 1.57 to 2.53 was observed by Haberl et al. [33] for 30 min. annealing at 450°C of unhydrogenated a-Si prepared by (silicon) ion implantation, thus showing the same trend as we observe.

4. Discussion

One major result of the present article is that after annealing at 450°C the HW grown a-Si-H film is divided into two parts. The top part exhibits a H out-diffusion profile characteristic for rather dense a-Si:H and an 1/MRO parameter close to device-grade a-Si:H, whereas silicon-bound hydrogen completely disappeared in the substrate-near part and 1/MRO indicates low order as in dehydrogenated a-Si:H. This finding may be of technological importance for the fabrication of liquid phase crystallized solar cells since it shows that a suitable microstructure can facilitate the out-diffusion of hydrogen which is a crucial step before laser liquid phase crystallization of a-Si:H. Both the asymmetry of H and MRO in the 450°C annealed material show that a microstructural change took place in the 450°C annealing step. The experimental results suggest that in the lower (substrate-near) part of the film interconnected voids are present. As a mechanism of void formation, we think of a shrinkage of the material upon H release which is likely inhomogeneous near the substrate [9].

If interconnected voids are thus generated near the substrate and hydrogen is fully depleted in this range, one may ask how the hydrogen leaves the film and where it is going. Several paths are conceivable. Some diffusing atomic hydrogen (in dense material) is likely to go into small isolated voids forming H_2 there, as detected by low temperature specific heat experiments [34]. Here, it was found that by annealing the amount of molecular H in such voids increases. This molecular hydrogen would not show up in the Raman spectra in the investigated frequency range.

Once in molecular form and likely under pressure, hydrogen may leak out furthermore via cracks and pinholes through the denser hydrogenated surface layer of the 450°C annealed material. We consider the diffusion of H_2 into the Corning substrate as rather unlikely because the ONO layer acts as a barrier. Reasons are (i) the high thermal stability of hydrogen in silicon nitride [12] which represents the central layer of the ONO, and (ii) that the oxide layers provide fast lateral diffusion paths, as discussed below. Furthermore, according to Norton [35] the H permeation coefficient in Corning glass is expected to be low because of a high content of boron/aluminum oxide.

There are two processes which may provide fast lateral out-diffusion of molecular H formed by annealing. One could go via the oxide layer of the ONO, the other which we consider more likely, via interconnected voids.

Considering H diffusion in amorphous SiO_2, Lee et al. [36] give for the Arrhenius dependence of diffusion the expression $D = 5.65 \times 10^{-4}$ cm^2/s exp (-0.45 eV/kT). This gives at 450°C annealing a H diffusion coefficient of 4.06×10^{-7} cm^2/s. At an annealing time of 4h, a H diffusion length of 0.15 cm is obtained, i.e. of the scale of the sample size which is 2 x 2 cm^2. Little information exists about the H_2 diffusion in interconnected voids in amorphous silicon apart that it is considered to be a fast process. However, a material with diffusion of molecular hydrogen is porous silicon. For the hydrogen diffusion coefficient in such material, the dependence $D = 9.2 \times 10^{-3}$ exp (-0.34 eV/kT) has been published [37]. This latter dependence gives at 450°C a H diffusion coefficient of 3.9×10^{-5} cm^2/s and for 4 hours annealing a diffusion length of 1.5 cm is calculated, again of dimension of the investigated sample.

Our (tentative) explanation for the disappearance of H near the substrate is based on the observed void formation in a-Si:H films on annealing, as detected by effusion of implanted He [9] and by positron annihilation experiments [8]. As some hydrogen (H_2) diffuses (laterally) out near the a-Si:H/ONO interface by one or both of these lateral

diffusion processes, the substrate-near part of the film gets depleted of hydrogen and will contract, as the a-Si:H density increases when hydrogen is released. Due to the sticking to the substrate, however, the film cannot contract laterally in the substrate-near range . It was proposed that such an inhomogeneous contraction leads to the formation of voids [9]. For thick films, such void formation is predominantly expected to take place in the substrate-near range while the surface-near part presumably contracts homogeneously without much void-formation. In the substrate-near part of the film, Si bound atomic H (present from the deposition process) is expected to diffuse only over a short diffusion length to the grain surfaces where it forms H_2 in a surface desorption process [7, 38]. Molecular H is then expected to diffuse rapidly through the interconnected voids out of the material, not only directly at the interface to the ONO but throughout the substrate near part of the film. However, very likely H_2 motion through interconnected voids must be considered as migration via capillaries of different dimensions involving interaction with (e.g.) silicon dangling bonds which can adsorb and desorb hydrogen. Thus, depending on microstructure, quite different temperature dependences of H_2 diffusion may apply. E.g., the Arrhenius dependence $D \approx 10^{-3}$ cm^2/s exp (-1.0 eV/kT) reported by Street and Tsai [39] for diffusion of hydrogen in a-Si:H with a columnar microstructure may also be due to diffusion by hydrogen molecules. This dependence would lead to a H diffusion coefficient at 450°C of $D \approx 10^{-10}$ cm^2/s and to a H diffusion length of $L \approx 24$ µm for 4 h annealing at that temperature. Thus, L would exceed the film thickness greatly and this could explain the observed depletion of hydrogen. While rapid H out-diffusion by H_2 molecules has been reported quite often for a-Si:H material deposited at low substrate temperature with high hydrogen concentrations [7] or for Si materials with pronounced void-related microstructure [18, 30], it has not been proposed to appear (to our knowledge) in high temperature annealing so far. While interconnected voids caused by excessive H incorporation, were found to disappear upon annealing and hydrogen release [7], the

present results suggest an appearance of interconnected voids upon annealing in regions of high network strain in a-Si:H in an environment of diffusing hydrogen. Film peeling is presumably related to this effect. While such a high temperature void generation is probably a new concept for amorphous silicon technology, it is not new for technology of crystalline silicon wafers, as the technique of "smart cut" is based on similar processes. "Smart cut" is known to involve (implanted) hydrogen, annealing, void (platelet) and interconnected void formation resulting finally in the lift-off of large areas of thin film silicon [40].

With regard to the MRO microstructure of a-Si:H, dependences on deposition method [21], deposition temperature [21, 24], and doping [19, 20] have been reported. Notable is also a relation between MRO and light-induced degradation reported by Ito and Kondo [22]. We find for the MRO parameter changes upon annealing and dependences on depth which, to our knowledge have not been reported before. By associating low 1/MRO parameter values with the presence of strained Si-Si bonds and rather high 1/MRO values with an expected presence of rather relaxed Si-Si bonds, we can qualitatively explain most obtained results. Thus, the expectation that near the film surface bonds are more relaxed and towards the interface more strained is supported by our data. Moreover, we find for the 450°C annealed material a correlation between hydrogen release and a decreasing reciprocal medium range order parameter. Thus, according to the present results the medium range order appears to be an interesting parameter for a-Si:H network characterization. Much more work, however, appears necessary to better understand the MRO microstructure and its dependence on material properties (related to deposition parameters), annealing and hydrogen.

With regard to the intended silicon crystallization process, there are reports that the presence of H affects this process by (e.g.) decohesion/ delamination and, therefore, an at least 12 hours annealing process up to 550°C was proposed [6]. Our results show

that our hot wire grown a-Si:H is a material that loses its hydrogen quite rapidly by annealing at 450 – 550°C. After annealing at 550°C for effectively 4 hours (neglecting the preceding annealing steps at lower temperatures) little silicon-bonded hydrogen remains in a 4500 nm thick film. This result shows that the long annealing time so far required to remove the hydrogen from thick a-Si:H precursor layers aimed for liquid phase crystallized thin film silicon solar cells may get reduced by developing suitable a-Si:H films which release hydrogen at a reduced annealing temperature.

We note that the void-related microstructure of plasma-grown and hot-wire grown a-Si:H seems to be quite different. For films of about 10 at.% of hydrogen, Mahan et al. [41] and Williamson [42] noted a higher concentration of voids in hot wire grown than in plasma-grown a-Si:H. To similar conclusions came Beyer et al. [43, 44] studying the effusion of implanted helium. This higher concentration of deposition-related voids which likely reduce network strain and which can take up diffusing hydrogen may stabilize the thick HW grown films so that they are not peeling while an interconnected void system is formed in the substrate-near range at high annealing temperatures. We think that by optimizing the HW deposition conditions an economically viable material may be found for the present purpose. We note that the rather high deposition rates achieved with HW growth [3, 4] would also favor economy.

5. Conclusions

The results show that a (rather) complete and (moderately) fast H removal from thick (HWCVD-grown) a-Si:H films is possible under the applied annealing conditions without peeling effects. Upon annealing, the hydrogen depth profile is not (predominantly) determined by H out-diffusion from a dense material. Rather, the observed depletion of hydrogen in the substrate-near part after annealing at 450°C implies rapid H diffusion and a change in material microstructure. We attribute this

microstructural change to the formation of interconnected voids, presumably due to inhomogeneous shrinking effects. Thus, void-related microstructure likely leads to the (rather) complete removal of hydrogen in the substrate-near part at annealing temperatures (≈ 4 hours) near 450°C and in the whole film after annealing (≈ 4 hours) at 550 °C. We presume that the higher concentration of voids in HWCVD a-Si:H (compared to plasma-grown dense a-Si:H) reduces network strain, prevents peeling and favors the formation of the interconnected void structure. In the dehydrogenated material, the reciprocal MRO microstructure parameter near the film-substrate interface is rather low, supporting the presence of reconstructed (strained) Si-Si bonds. For the substrate-near part of the film, the observed direct correlation between 1/MRO and hydrogen concentration after the annealing up to a temperature of 450°C can be explained by the reconstruction of strained Si-Si bonds when hydrogen is released. The dependence of MRO on hydrogen density and depth suggests that MRO, in particular the reciprocal MRO, is a meaningful and useful parameter characterizing amorphous silicon thin films. In summary, the results show that HW grown thick a-Si:H films can be well suited as precursor layers for liquid phase crystallized silicon solar cells on glass.

Acknowledgements

The authors would like to thank Markus Hülsbeck for his support with the Raman measurements. A helpful discussion with Prof. R. Carius is gratefully acknowledged.

The work was supported by the European Union and the State of North Rhine-Westphalia (Up-LLPC Project ID EFRE0800-561).

References

[1] M.A. Green, P.A. Basore , N. Chang, D. Clugston, R. Egan, R. Evans, D. Hogg, S. Jarnason, M. Keevers, P. Lasswell, J. O´Sullivan, U. Schubert, A. Turner, S.R. Wenham, T. Young, Crystalline silicon on glass (CSG) thin-film solar cell modules Solar Energy 77(6) (2004) 857-863.

[2] C. Thi Trinh, N. Preissler, P. Sonntag, M. Muske, K. Jäger, M. Trahms, R. Schlatmann, B. Rech, D. Amkreutz, Potential of interdigitated back-contact silicon heterojunction solar cells for liquid phase crystallized silicon on glass with efficiency above 14%, Sol. Energy Mater. Sol. Cells 174 (2018) 187-195. https://doi.org/10.1016/j.solmat.2017.08.042.

[3] A.H. Mahan, Y. Xu, J.D. Perkins, L.M. Gedvilas, R.S. Crandall, B.P. Nelson, D.L. Williamson, W. Beyer and J.D. Cohen, The properties of a-Si:H films and devices deposited by hot wire CVD at ultra high deposition rates, MRS Symp. Proc. 664 (2001) A3.3.

[4] A.H. Mahan, Y. Xu, D.L. Williamson, W. Beyer, J.D. Perkins, M. Vanecek, L.M. Gedvilas and B.P. Nelson, Structural properties of hot-wire a-Si:H deposited at rates in excess of 100Å/s. J. Appl. Phys. 90 (2001) 5038-5047.

[5] Z. Said-Bacar, P. Prathap, C. Cayron, F. Mermet, Y. Leroy, F. Antoni, A.Slaoui, E. Fogarassy, CW laser induced crystallization of thin amorphous silicon films deposited by EBE and PECVD, Appl. Surf. Sci. 258 (2012) 9359-9365.

[6] O. Gabriel, T. Frijnts, S. Calnan, S. Ring, S. Kirner, A. Opitz, I. Rothert, H. Rhein, M. Zelt, K. Bhatti, J-H Zollondz, A. Heidelberg, J. Haschke, D. Amkreutz, S. Gall, F. Friedrich, B. Stannowski, B. Rech, R. Schlatmann, PECVD Intermediate and absorber

layers applied in liquid-phase crystallized Si solar cells on glass substrates, IEEE J. Photovolt. 4 (6) (2014) 1343-1348.

[7] W. Beyer, H. Wagner, The role of hydrogen in a-Si:H - results of evolution and annealing studies, J. Non-Cryst. Solids 59-60 (1983) 161-168. https://doi.org/10.1016/0022-3093(83)90547-1.

[8] M. Schouten, The nanostructure of hydrogenated amorphous silicon examined by means of thermal annealing and light soaking, Master Thesis, TU Delft, The Netherlands, 2013.

[9] W. Beyer, W. Hilgers, D. Lennartz, F.C. Maier, N.H. Nickel, F. Pennartz, P. Prunici, Effect of Annealing on Microstructure in (Doped and Undoped) Hydrogenated Amorphous Silicon Films, MRS Symp. Proc. 1666 (2014) 667. https://doi.org/10.1557/opl.2014.667.

[10] C. Maurer, S. Haas, W. Beyer, F.C. Maier, U. Zastrow, M. Hülsbeck, U. Breuer, U. Rau, Application of Raman spectroscopy for depth-dependent evaluation of the hydrogen concentration of amorphous silicon, Thin Solid Films 653 (2018) 223-228. https://doi.org/10.1016/j.tsf.2018.02.037.

[11] S. R. Elliott, Medium-range structural order in covalent amorphous solids, Nature 354 (1991) 445-452.

[12] A. Hofmann, S. Kambor, C. Schmidt, D, Grambole, J. Rentsch, S.W. Glunz, R. Preu, PECVD-ONO: A New Deposited Firing Stable Rear Surface

Passivation Layer System for Crystalline Silicon Solar Cells, Advances in Optoelectronics (2008), art. no.485467.

[13] J. Dore, R. Evans, B. D. Eggleston, S. Varlamos, M.A. Green, Intermediate Layers for Thin-Film Polycrystalline Silicon Solar Cells on Glass Formed by Diode Laser Crystallization, MRS Symp. Proc.1426 (2012) 63- 68.

[14] Sina Kurth, Raman-spektroskopische Untersuchung des Wasserstoffgehalts und der Mikrostruktur von a-Si:H Präkursorschichten für flüssigphasenkristallisierte c-Si Solarzellen (Raman-spectroscopic analysis of the hydrogen content and the microstructure of a-Si:H precursor layers for liquid phase crystallized c-Si solar cells) Bachelor Arbeit, Cologne, Germany,2018, unpublished.

[15] P. Vora, S.A. Solin, P. John, Raman scattering from pristine and oxidized polysilanes, Phys. Rev. B 29 (1991) 3423-3429.

[16] M. Cardona, Vibrational Spectra of Hydrogen in Silicon and Germanium, Phys. Status Solidi B 118 (1983) 463-481.
https://doi.org/10.1002/pssb.2221180202.

[17] H. Wagner and W. Beyer, Reinterpretation of the Silicon-Hydrogen Stretch Frequencies in Amorphous Silicon, Solid State Commun. 48 (1983) 585- 587.

[18] W. Beyer, Diffusion and evolution of hydrogen in hydrogenated amorphous and microcrystalline silicon, Sol. Energy Mater. Sol. Cells 78 (2003) 235-267.
https://doi.org/10.1016/S0927-0248(02)00438-5.

[19] A.P. Sokolov, A.P. Shebanin, O.A. Golikova, M.M. Mezdrogina, Structural order in amorphous silicon and its alloys: Raman spectra and optical gap, J. Non-Cryst. Solids 137-138 (1991) 99-102.
https://doi.org/10.1016/S0022-3093(05)80066-3.

[20] O. A. Golikova and V. K. Kudoyarova, Defects and short and medium-range order in the structural network of hydrogenated amorphous silicon, Semiconductors 32 (1998) 779- 781.

[21] G. Morell, R.S. Katiyar, S.Z. Weisz, H. Jia, J. Shinar, and I. Balberg, Raman study of the network disorder in sputtered and glow discharge a-Si:H films. J. Appl. Phys. 78 (1995) 5120-5125.

[22] M. Ito, M. Kondo, Systematic Study of Photodegradation of Tailored Nanostructure Si Solar Cells by Controlling Their Medium Range Order, Jpn. J. Appl. Phys. 45 (2006) 230-232.
DOI: 10.1143/JJAP.45.L230.

[23] F. Köhler, Zur Mikrostruktur siliziumbasierter Dünnschichten für die Photovoltaik, Ph.D Thesis, RWTH Aachen University, Germany, 2012.

[24] P- Danesh, B. Pantchev, K. Antonova, F. Liarokapis, B. Schmidt, D. Grambole and J. Baran, Hydrogen bonding and structural order in hydrogenated amorphous silicon prepared by hydrogen-diluted silane, J. Phys. D Appl. Phys. 37 (2004) 249-254.

[25] L. Houben, M. Luysberg, P. Hapke, R. Carius, F. Finger & H. Wagner,

Structural properties of microcrystalline silicon in the transition from highly crystalline to amorphous growth, Philosophical Magazine A, 77(6) (1998) 1447-1460.
DOI: 10.1080/01418619808214262

[26] M. Reinelt, S. Kalbitzer, G. Müller, The diffusion of hydrogen in amorphous silicon, J. Non-Cryst. Solids 59-60 (1983) 169-172.
https://doi.org/10.1016/0022-3093(83)90548-3.

[27] C. Maurer, W. Beyer, M. Hülsbeck, U. Breuer, U. Rau, S. Haas, Impact of laser treatment on hydrogenated amorphous silicon properties, Adv. Eng. Mater., 22(6) (2020) 1901437.
DOI: 10.1002/adem.201901437

[28] W. Beyer, H. Wagner, Determination of the hydrogen diffusion coefficient in hydrogenated amorphous silicon from hydrogen effusion experiments, J. Appl. Phys. 53 (1982) 8745-8750.
https://doi.org/10.1063/1.330474.

[29] D.E. Carlson and C.W. Magee, A SIMS analysis of deuterium diffusion in hydrogenated amorphous silicon, Appl. Phys. Lett. 33 (1978) 81.

[30] W. Beyer, Hydrogen Phenomena in Hydrogenated Amorphous Silicon, in: Semiconductors and Semimetals 61, N.H. Nickel, ed. (Academic, San Diego, 1999) p.165-239.

[31] B. Pantchev, P. Danesh, E, Liarokapis, B. Schmidt, J. Schmidt, and D. Grambole, Effect of Post-Hydrogenation on the Structural Properties of Amorphous Silicon Network, Jap. J. Appl. Phys. 43 (2004) 454-458.

[32] W. Beyer, U. Breuer, R. Carius, W. Hilgers, D. Lennartz, F.C. Maier, N.H. Nickel, F. Pennartz, P. Prunici, and U. Zastrow, Influence of hydrogen concentration on void-related microstructure in low hydrogen amorphous and crystalline silicon materials, Can. J. Phys. 92 (2014) 700–704.
dx.doi.org/10.1139/cjp-2013-0555

[33] B. Haberl, S.N. Bogle, T. Li, I. McKerracher, S. Ruffell, P. Munroe, J.S. Williams, J.R. Abelson, and J.E. Bradby, Unexpected short- und medium range atomic structure of sputtered amorphous silicon upon thermal annealing, J. Appl. Phys. 110 (2011) 096104-01-03.

[34] H. v. Löhneysen, H.J. Schink, W. Beyer, Direct Experimental Evidence for Molecular Hydrogen in Amorphous Si:H, Phys. Rev. Lett. 52 (1984) 549.

[35] F.J. Norton, Helium diffusion through glass, J. Am. Ceram. Society 36 (1953) 90-96.

[36] R. W. Lee, R. C. Frank, and D. E. Swets, Diffusion of Hydrogen and Deuterium in Fused Quartz, J. Chem. Phys. 36, (1962) 1062.
https://doi.org/10.1063/1.1732632

[37] T. Dzhafarov and S. A. Yuksel, Diffusion of hydrogen in porous silicon-based gas sensors, J. of Porous Media 13(2) (2010) 97 -1029.

[38] W. Beyer, Hydrogen incorporation, stability and release effects in thin film silicon, Phys. Status Solidi A 213 (7) (2016) 1661-1674. https://doi.org/10.1002/pssa.201532976.

[39] R.A. Street and C.C.Tsai, Dependence of hydrogen diffusion on growth conditions in hydrogenated amorphous silicon, Philos. Mag. B57 (1988) 663-669.

[40] B. Aspar, M. Bruel, H. Moriceau, C. Maleville, T. Poumeyrol, A.M. Papon, A. Claverie, G. Benassayag, A.J. Auberton-Hervé, T. Barge, Basic mechanisms involved in the Smart-Cut® process, Microelectron. Eng. 36 (1997) 233–240.

[41] A.H. Mahan, Y. Chen, D.L. Williamson, and G.D. Mooney, Deposition of device quality, low H content a-Si:H by the hot wire technique, J. Non-Cryst. Solids 137-138 (1991) 657-660.

[42] D. L. Williamson, Nanostructure of a-Si:H and related materials by small-angle x-ray scattering, MRS Symp. Proc. 377 (1995) 251-262.

[43] W. Beyer, W. Hilgers, D. Lennartz, F. Pennartz, P. Prunici, Isolated voids in amorphous silicon and related materials measured by effusion of implanted helium, MRS Symp. Proc. 1426 (2012) 341-346.

[44] W. Beyer, W. Hilgers, D. Lennartz, F.C. Maier, N.H. Nickel, F. Pennartz, P. Prunici, Microstructure characterization of amorphous silicon films by effusion measurements of implanted helium, MRS Symp. Proc. 1536 (2013) 175-180.

Figure 1:	Annealing procedure of investigated samples. Sample 1: untreated; sample 2: heated up to 450 °C; sample 3: heated up to 550 °C
Figure 2:	Raman signal between 1800 and 2300 cm^{-1} of the untreated sample. The sum of the two integrals of fitted Gaussians centered near 2000 cm^{-1} and 2100 cm^{-1} provide a measure of the normalized hydrogen intensity
Figure 3:	(a) Raman spectrum of the amorphous silicon Si-Si vibrations between 80 and 560 cm^{-1}. The assignment to phonon modes (TA, LA, LO, TO) is indicated. We define the reciprocal MRO parameter in analogy to [23] by $1/MRO = (2\ I_{TO}\ /2)\ /\ I_{TA}$. (b) Raman spectra of the as-deposited sample and the samples heated up to 450 °C and 550 °C, measured at a depth of about 2650 nm
Figure 4:	Normalized H intensity (squares) and H microstructure parameter (triangles) as a function of layer depth for (a) the untreated sample and (b) the sample heated up to 450 °C
Figure 5:	Reciprocal MRO parameter depth profiles of the untreated sample (a) and the sample heated to 450 °C (b)
Figure 6:	Fig. 6: Correlation between reciprocal MRO parameter (1/MRO) and normalized Raman H intensity in in the substrate near part of the a-Si:H film heated up to 450°C.
Figure 7:	Depth profile of the reciprocal MRO parameter for the sample heated up to 550 °C

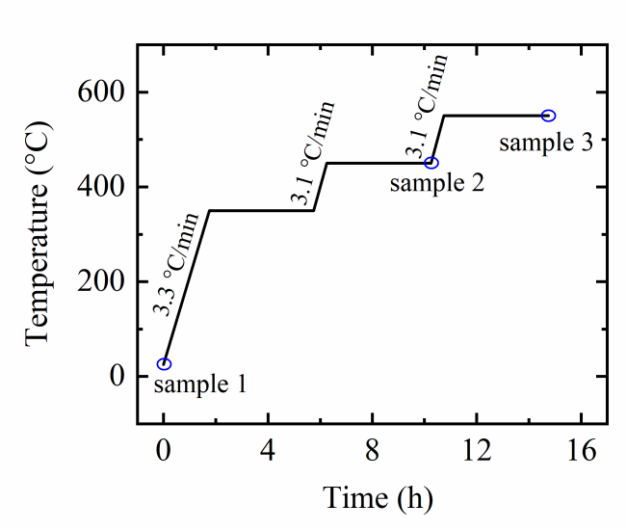

Fig. 1: Annealing procedure of investigated samples. Sample 1: untreated; sample 2: heated up to 450 °C; sample 3: heated up to 550 °C

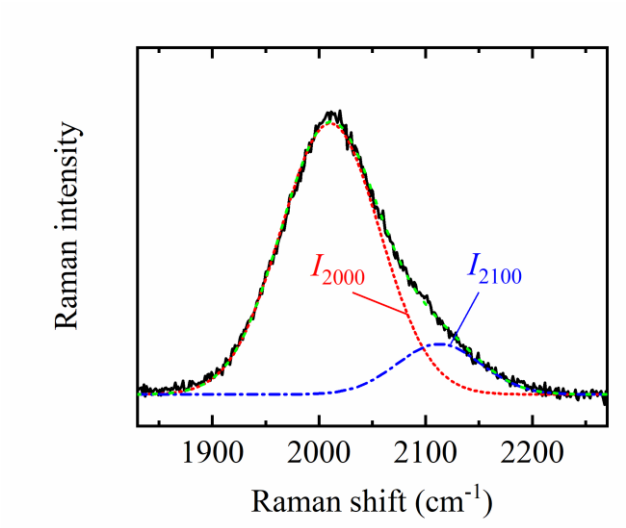

Fig. 2: Raman signal between 1800 and 2300 cm^{-1} of the untreated sample. The sum of the two integrals of fitted Gaussians centered near 2000 cm^{-1} and 2100 cm^{-1} provide a measure of the normalized hydrogen intensity

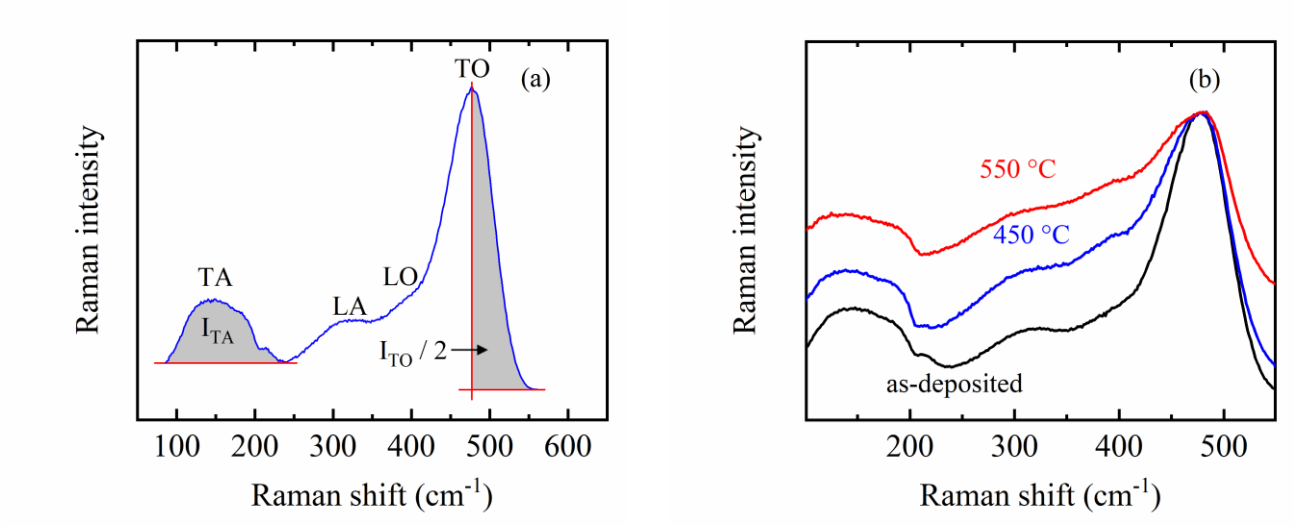

Fig. 3: (a) Raman spectrum of the amorphous silicon Si-Si vibrations between 80 and 560 cm^{-1}. The assignment to phonon modes (TA, LA, LO, TO) is indicated. We define the reciprocal MRO parameter in analogy to [23] by 1/MRO = (2 I_{TO} /2) / I_{TA} (b) Raman spectra of the as-deposited sample and the samples heated up to 450 °C and 550 °C, measured at a depth of about 2650 nm

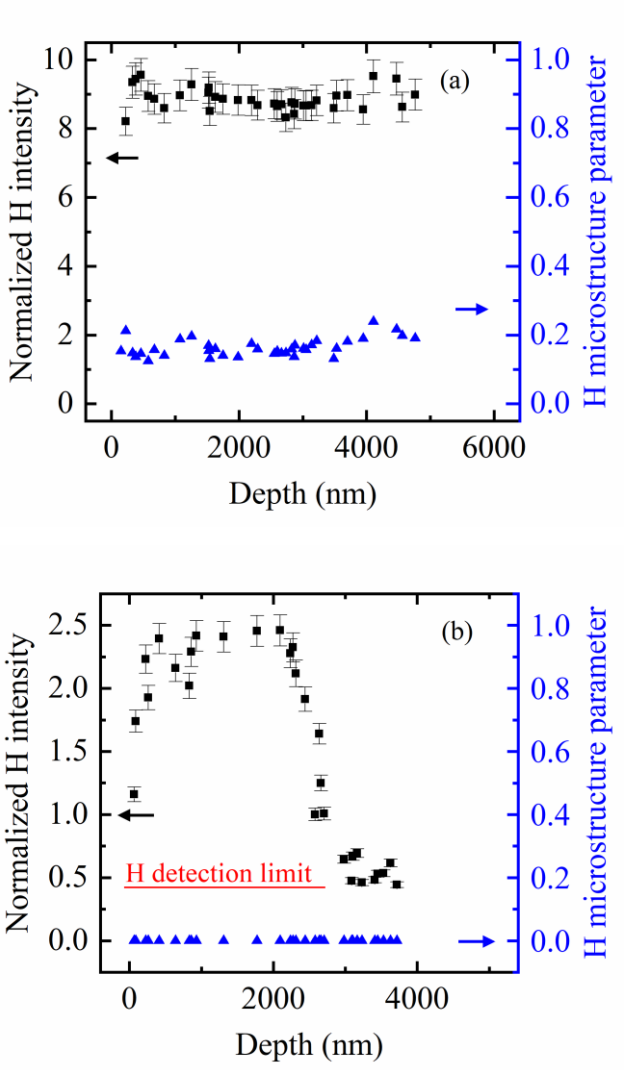

Fig. 4: Normalized H intensity (squares) and H microstructure parameter (triangles) as a function of layer depth for (a) the untreated sample and (b) the sample heated up to 450 °C

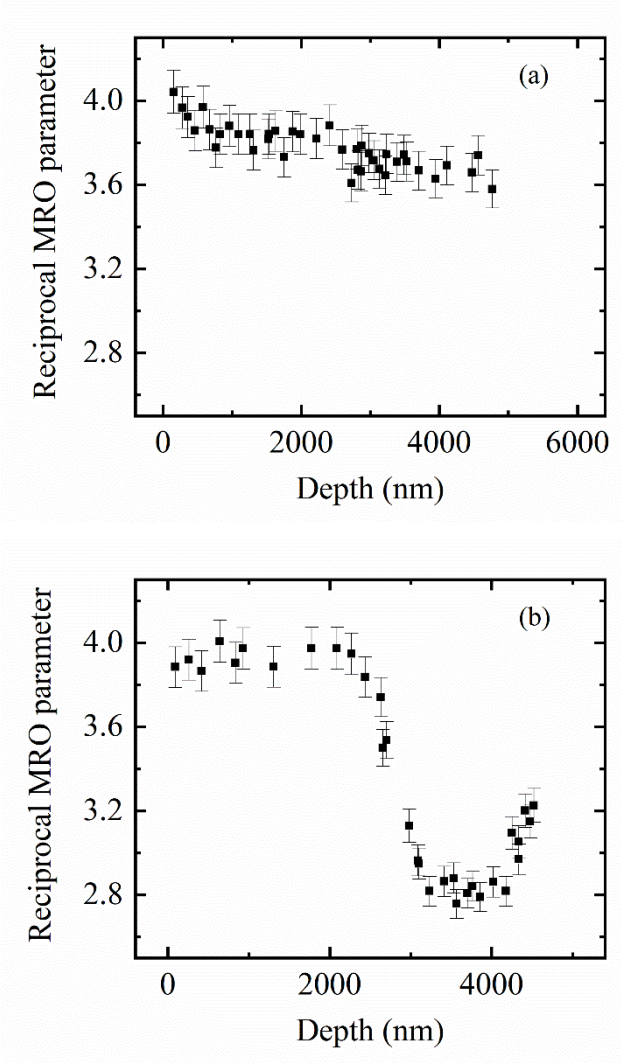

Fig. 5: Depth profiles of the reciprocal MRO parameter of the untreated sample (a) and the sample heated to 450 °C (b)

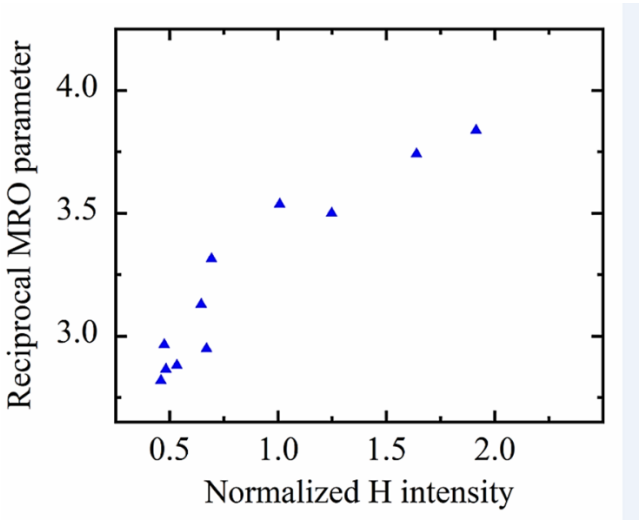

Fig. 6: Correlation between reciprocal MRO parameter and normalized Raman H intensity in in the substrate near part of the a-Si:H film heated up to 450 °C.

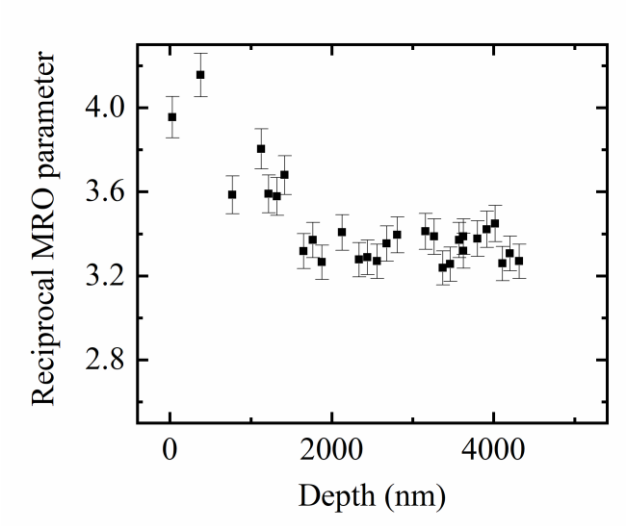

Fig. 7: Depth profile of the reciprocal MRO parameter for the sample heated up to 550 °C